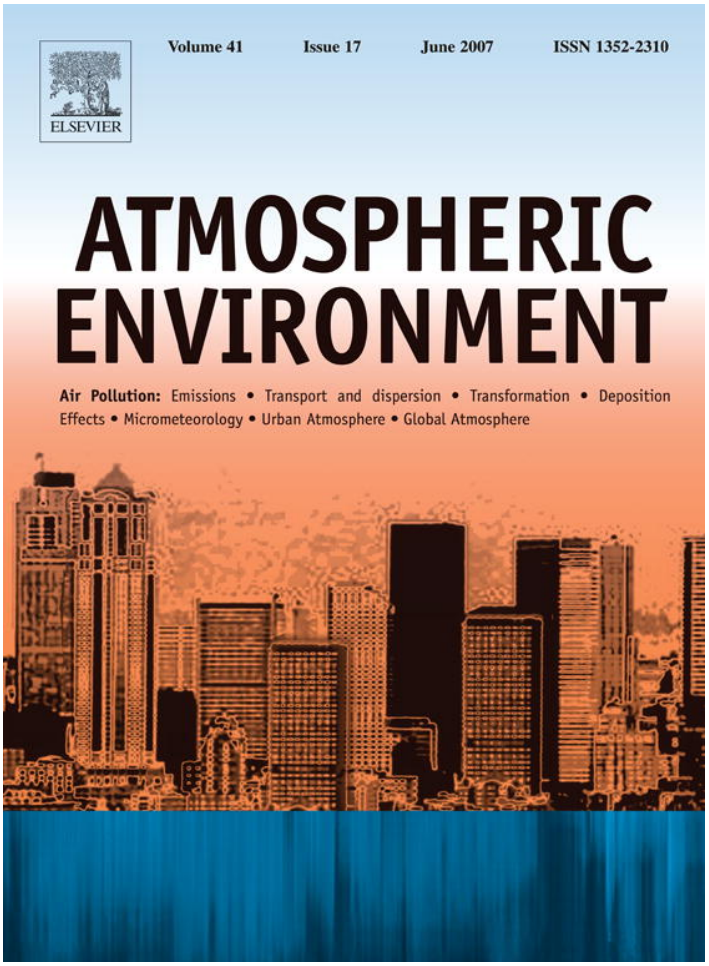

Available online at www.sciencedirect.com
ScienceDirect
Atmospheric Environment 41 (2007) 3577–3589
ATMOSPHERIC ENVIRONMENT
www.elsevier.com/locate/atmosenv

# Chemical composition of aerosols during a major biomass burning episode over northern Europe in spring 2006: Experimental and modelling assessments

Sanna Saarikoski*, Markus Sillanpää, Mikhail Sofiev, Hilkka Timonen, Karri Saarnio, Kimmo Teinilä, Ari Karppinen, Jaakko Kukkonen, Risto Hillamo

*Finnish Meteorological Institute, Air Quality, P.O. Box 503, FI-00101 Helsinki, Finland*

Received 26 September 2006; received in revised form 14 December 2006; accepted 21 December 2006

**Abstract**

The long-range transported smokes emitted by biomass burning had a strong impact on the $PM_{2.5}$ mass concentrations in Helsinki over the 12 days period in April and May 2006. To characterize aerosols during this period, the real-time measurements were done for $PM_{2.5}$, $PM_{2.5–10}$, common ions and black carbon. Moreover, the 24-h $PM_1$ filter samples were analysed for organic and elemental carbon (OC and EC), water-soluble organic carbon (WSOC), ions and levoglucosan. The Finnish emergency and air quality modelling system SILAM was used for the forecast of the $PM_{2.5}$ concentration generated by biomass burning. According to the real-time $PM_{2.5}$ data, the investigated period was divided into four types of PM situations: episode 1 (EPI-1; 25–29 April), episode 2 (EPI-2; 1–5 May), episode 3 (EPI-3; 5–6 May) and a reference period (REF; 24 March–24 April). EPI-3 included a local warehouse fire and therefore it is discussed separately. The $PM_1$ mass concentrations of biomass burning tracers—levoglucosan, potassium and oxalate—increased during the two long-range transport episodes (EPI-1 and EPI-2). The most substantial difference between the episodes was exhibited by the sulphate concentration, which was 4.9 ($\pm$1.4) $\mu g\,m^{-3}$ in EPI-2 but only 2.4 ($\pm$0.31) $\mu g\,m^{-3}$ in EPI-1 being close to that of REF ($1.8 \pm 0.54\,\mu g\,m^{-3}$). The concentration of particulate organic matter in $PM_1$ was clearly higher during EPI-1 ($11 \pm 3.3\,\mu g\,m^{-3}$) and EPI-2 ($9.7 \pm 4.0\,\mu g\,m^{-3}$) than REF ($1.3 \pm 0.45\,\mu g\,m^{-3}$). The long-range transported smoke had only a minor impact on the WSOC-to-OC ratio. According to the model simulations, MODIS detected the fires that caused the first set of concentration peaks (EPI-1) and the local warehouse fire (EPI-3), but missed the second one (EPI-2) probably due to dense frontal clouds.


*Keywords:* Aerosols; Biomass burning; Chemical composition; Long-range transport

## 1. Introduction

Biomass burning has considerable regional and global impacts, on both the chemical properties of the atmosphere and the radiative balance of the Earth (Andreae and Merlet, 2001). Aerosols perturb the climate through the backscattering and absorbing

*Corresponding author. Tel.: +358 9 1929 5508; fax: +358 9 1929 5403.
*E-mail address:* sanna.saarikoski@fmi.fi (S. Saarikoski).

1352-2310/$ - see front matter © 2007 Elsevier Ltd. All rights reserved.
doi:10.1016/j.atmosenv.2006.12.053

of incident sunlight (direct effect) and the modification of cloud properties (indirect effect) (Seinfeld and Pandis, 1998). Substantial populations throughout the world also suffer each year from smokes originated from local and distant wild land and agricultural fires (e.g., Duclos et al., 1990; Heil and Goldammer, 2001). The smoke from biomass burning contains numerous gaseous (e.g., CO and VOCs) and particulate compounds (e.g., PAHs and other organics) that are known to be hazardous to human health. Metzger et al. (2004) have reported that the mass concentrations of elemental carbon (EC) and organic carbon (OC) in particles with diameter smaller than 2.5 μm (fine particles, $PM_{2.5}$) were significantly associated with emergency department visits in hospitals due to cardiovascular diseases.

Airborne submicron particles originate from various combustion processes or are formed through secondary processes from their precursor gases in the atmosphere. On a global basis, biomass burning is the dominant source of particulate organic carbon (Debell et al., 2004). The quantity and composition of biomass combustion particles depend on various factors, such as the composition and structure of the fuel, terrain, weather and the duration of flaming versus smouldering (Conny and Slater, 2002). Long-range transported smoke emitted from biomass burning contains hundreds of different organic compounds, EC, secondary inorganic ions, nutrient elements and trace metals (e.g., Fine et al., 2001). In previous studies, potassium (e.g., Watson et al., 1994), oxalate (Jaffrezo et al., 1998) and levoglucosan (Simoneit et al., 1999) in the particle phase have been used as biomass combustion tracers. Of these, the only specific tracer of biomass combustion particles is levoglucosan that is formed in the thermal breakdown of cellulose (Fraser and Lakshmanan, 2000).

As the mass concentrations of fine particles are commonly lower in Nordic countries compared with, e.g., those in Central Europe (Sillanpää et al., 2006), long-range transport can have a remarkable impact on the PM levels under certain conditions (Pakkanen et al., 2001; Karppinen et al., 2004). The long-range transport of emissions from wild land fires from the Baltic countries, Belarus, Ukraine and Russia raises the PM concentrations in Finland frequently during spring and summer (Niemi et al., 2004, 2005; Sillanpää et al., 2005).

In contrast to the episodes described in the earlier studies, the biomass smoke episode observed in April and May 2006 was exceptionally long, lasting about 12 days. The model computations of this study showed that during part of this time, the polluted air masses were long-range transported up to the high Arctic latitudes. The available data from state-of-the-art chemical and physical characterization methods enabled an extensive chemical characterization of the episode in order to provide data for the testing and evaluation of models, the estimation of the adverse health effects caused by the fire plumes and the assessment of climatic effects.

## 2. Experimental

### 2.1. Measurement site

The measurements of this study were performed in Helsinki, Finland, at an urban background station SMEAR III (60°20′N, 24°97′E, 26 m above sea level, for more details see http://www.atm.helsinki.fi/SMEAR/). The site is located in the campus area of the University of Helsinki, 5 km northeast from the centre of Helsinki. The most important local source of fine particulate matter is vehicular traffic; however, the contribution of biomass combustion may be substantial, especially in winter.

### 2.2. Real-time measurements

#### 2.2.1. TEOM

The concentrations of $PM_{2.5}$ and $PM_{2.5–10}$ were measured with two Tapered Element Oscillating Microbalance units (TEOM©, Rupprecht & Patashnick; Allen et al., 1997; Patashnick and Rupprecht, 1991). The size ranges were controlled using a virtual impactor (VI; Loo and Cork, 1988). The TEOM 1400a was measuring the fine particle fraction from the major flow of the VI (15 L $min^{-1}$) at 30 °C, whereas the TEOM 1400 was connected to the minor flow of the VI (1.6 L $min^{-1}$) to measure coarse fraction at 50 °C. The TEOM 1400a was equipped with a Filter Dynamics Measurement System (FDMS). Briefly, the FDMS has a Sample Equilibration System (SES) dryer to remove relative humidity of the ambient air. Also, every 6 min the air is passed through a filter to get a particle-free sample into the TEOM. During that phase, the loss of mass from the TEOM is measured and considered as a semi-volatile particular matter. Based on the comparison of the TEOM with the filter measurements conducted previously in Finland, the

uncertainty of the TEOM was estimated to be 10% for non-volatile $PM_{2.5}$ and for $PM_{2.5-10}$. Including semi-volatile $PM_{2.5}$, the TEOM gave an average of 11% larger results than those obtained from the $PM_{2.5}$ filter measurements.

#### 2.2.2. PILS-IC

The ion composition of aerosol particles was measured continuously using a PILS-IC system. The system consists of a VI, Particle-Into-Liquid-Sampler (PILS, Orsini et al., 2003), two Dionex 2000 ion chromatograph systems (cation and anion analysis) and an 8-channel peristaltic pump. The VI, modified from the design of Loo and Cork (1988), was connected to the PILS so that only particles smaller than 1 μm (major flow; 15 L $min^{-1}$) were sampled. Cation analyses (sodium, ammonium, potassium, magnesium and calcium) were made using a CG12A/CS12A column with an electrochemical suppressor (CSRS ULTRA II, 4 mm). Anion analyses (chloride, nitrate, sulphate and oxalate) were made using a AG11/AS11 column with electrochemical suppression (ASRS ULTRA II, 4 mm). Lithium fluoride was used as an internal standard. The detection limit for the measured ions was in the range 0.005–0.010 μg $m^{-3}$, the value depending on the ion analysed. The time resolution of the PILS-IC system was 15 min. The data from the PILS-IC was used only for qualitative analysis in this study.

#### 2.2.3. Aethalometer

Black carbon was measured with a 5-min resolution using a single-wavelength aethalometer (AE-16, Magee Scientific, wavelength 880 μm; Hansen et al., 1984). The aethalometer was equipped with a cyclone that removed particles larger than 2.5 μm in aerodynamic diameter. Black carbon equivalent concentrations were calculated from absorption measurements of the aethalometer using a mass absorption efficiency of 16.6 $m^2$ $g^{-1}$.

#### 2.2.4. Local meteorological measurements

Local meteorological data were measured at the station of Kaisaniemi that is located in central Helsinki, at a distance of 4 km south of the SMEAR III station. The meteorological parameters, visibility and relative humidity, were measured using a Vaisala weather sensor (Vaisala FD12P). The meteorological data were recorded with a temporal resolution of 10 min.

### 2.3. $PM_1$ sampling and analysis

#### 2.3.1. Sampling system

Filter samples were collected using a filter cassette system (Gelman Sciences) and two quartz fibre filters (Whatman Q-MA, 47 mm) back to back. To discriminate particles with an aerodynamic diameter larger than 1 μm, the four upper stages (8–11) of the Berner low-pressure impactor (BLPI; Berner and Lürzer, 1980) were used prior to the filter cassette at a flow rate of 80 L $min^{-1}$. The nominal cut-off diameter ($D_{50}$) for the stage 8 is 2 μm with a flow rate of 24.5 L $min^{-1}$. The sampling duration for $PM_1$ filters was mainly 24 h on working days and 72 h over weekends. The samplings were started at 9 a.m. local time. During the biomass burning episode, 12-h samples were collected in order to avoid filter overloads and minimize volatilization losses.

#### 2.3.2. Chemical analyses

$PM_1$ samples were cut into 1-$cm^2$ pieces and analysed for organic carbon, EC, water-soluble organic carbon (WSOC), water-soluble ions and levoglucosan. The water-insoluble organic carbon (WISOC) was calculated by subtracting the analysed WSOC from OC. The concentrations of OC and EC were determined with a thermal–optical transmission method (Birch and Cary, 1996) using an analyser manufactured by Sunset Laboratory Inc. The temperature programme was similar to the method developed by the National Institute for Occupational Safety and Health (NIOSH), except for the last temperature step in the helium phase that was decreased from 850 to 800 °C. The concentrations on the back-up filter were subtracted from those on the front filter. The mean (±SD) OC found on back-up filter was 12±3.2% and 4.2±1.8% of that found on the front filter for the reference period and the episodes, respectively. The uncertainty of the OC and EC analyses was estimated to be 10% and 20%, respectively. Particulate organic matter (POM) was obtained by multiplying OC by the factor of 1.6 (Turpin and Lim, 2001).

WSOC was analysed with a Total Carbon Analyzer equipped with a high-sensitive catalyst (TOC-$V_{CPH}$, Shimadzu). Samples were extracted by shaking the filter piece with 15 mL of Milli-Q water for 15 min. WSOC was determined by the Non-Purgeable Organic Carbon (NPOC) method, which measures non-volatile OC present in the sample.

Inorganic carbon (carbonates, hydrogen carbonates and dissolved carbon dioxide) was eliminated in NPOC method by acidifying the sample with 1% acid. Similar to the OC results, the concentrations of WSOC on the back-up filter were subtracted from those on the front filter. The mean ($\pm$SD) WSOC found on back-up filter was $26\pm15\%$ and $8.0\pm4.2\%$ of that found on the front filter for the reference period and the episodes, respectively. The uncertainty of the WSOC method was estimated to be 20%.

Ions (chloride, nitrate, sulphate, oxalate, sodium, ammonium, potassium, magnesium and calcium) were determined with two ion chromatographs (Dionex DX500). Samples were extracted with 5 mL of Milli-Q water and shaken for 10 min. The columns were similar to those in the PILS-IC system. Chemical suppression with sulphuric acid and electrochemical suppression were used for anions and cations, respectively. The uncertainty in the IC method is in the range 5–10%.

Levoglucosan was analysed with a liquid chromatograph coupled to an ion trap mass spectrometer (LC–MS, Agilent Technologies SL). Samples were extracted with a 2-mL mixture of tetrahydrofuran and water (1:1) in an ultrasonic bath for 30 min. The LC–MS method was similar to the method of Dye and Yttri (2005); however, the eluent was Milli-Q water with a flow rate of 0.1 mL $min^{-1}$. Two LC columns (Atlantis, 150 mm, Waters) were used at 7 °C. The ionization technique was electrospray and the monitored ion was $m/z$ 161. The uncertainty of the LC–MS method is estimated to be 20%.

### 2.4. Emission and atmospheric dispersion modelling

#### 2.4.1. Emissions of particulate matter from anthropogenic sources and fires

For the computation of the concentrations of primary particulate matter and sulphate in Europe, the European-scale emissions taken from the EMEP (European Monitoring and Evaluation Programme, http://www.emep.int) database were used. In order to evaluate the spatial coverage and the source strengths of fires, the near-real-time information regarding active fires was utilized. These data were extracted from the MODIS instrument onboard the NASA Aqua and Terra satellites (http://modis.gsfc.nasa.gov/). The emission fluxes of $PM_{2.5}$ were evaluated based on daily-averaged MODIS temperature anomalies (TAs). The procedures of GFEDv2 (Giglio et al., 2006) were utilized with a few amendments. TA is defined for each MODIS grid cell and each time instant as the difference of the observed temperature and the long-term average temperature for that location. The TAs are expected to provide the best available measure for the intensity of burning.

It was assumed that the fire intensity is directly proportional to the TA as registered by MODIS, with a spatial resolution of $1\times1\,km^2$. A spatially and temporally constant, empirically determined emission factor was used for all grid cells for which burning was detected. This emission factor was multiplied by the TAs. The fire intensity is expected to be higher during daytime, due to stronger atmospheric turbulence, stronger local winds and lower relative humidity. Therefore, a normalization function that describes the hourly diurnal variation of the fire intensity was introduced. This function is proportional to the solar radiation intensity in overcast conditions. The emission flux is equal to the product of the emission factor, TA and the diurnal normalization function. The final emission data set consists of sequential hourly $PM_{2.5}$ emission fluxes, aggregated to a spatial resolution of 20 km.

There was also a major warehouse fire in the centre of Helsinki on 5 May 2006. This fire influenced the $PM_{2.5}$ concentrations that were measured at the end of the time period considered in this study. This fire was also observed by MODIS as its emissions were treated on a resolution of $1\times1\,km^2$. The local fire affected, according to the real-time concentration measurements, one sample of $PM_1$ (from 5 May at 5:43 p.m. to 6 May at 2:00 p.m.).

#### 2.4.2. Atmospheric forward and inverse dispersion modelling

In March 2006, the Finnish Meteorological Institute started trial operational forecasts of the dispersion of particulate matter originated from biomass burning. The forecasting system utilizes as input data near-real-time satellite-based information on fires, and meteorological data from either the HIRLAM or ECMWF numerical weather prediction models. The atmospheric dispersion is modelled using the Finnish emergency and air quality modelling system SILAM (Sofiev et al., 2006, http://silam.fmi.fi). Its current operational version is based on a Lagrangian dispersion model

that applies an iterative advection algorithm and a Monte Carlo random-walk diffusion representation. It contains an extensive meteorological pre-processing module and is capable of both forward and adjoint simulations, of which the latter is used for delineating the source areas for some part of the episode. The model has been evaluated against the data of the European Tracer Experiment (Sofiev et al., 2006), as well as the data of the Chernobyl and Algeciras releases. For the purposes of this study, a re-analysis was conducted for the whole duration of the episode considered, i.e., from 20 April to 15 May 2006. For the current study, two sets of SILAM forecasts were used: (i) the concentrations of the fine particulate matter $PM_{2.5}$ originated from fires, and (ii) the anthropogenic primary $PM_{2.5}$ (emitted directly from industrial installations, cars, etc.) and sulphates. These concentrations can therefore be used for evaluating the fraction of $PM_{2.5}$ originated from fires compared with those originated from other kinds of anthropogenic sources.

## 3. Results

### 3.1. Real-time measurements

#### 3.1.1. $PM_{2.5}$ concentrations

The $PM_{2.5}$ concentrations increased on 25 April 2006 in Helsinki and remained at a significantly elevated level for almost 12 days. The $PM_{2.5}$ concentration measured by the TEOM has been presented in Fig. 1a. According to the $PM_{2.5}$ data, the period of elevated concentrations can be divided into three parts: episode 1 (EPI-1), episode 2 (EPI-2) and episode 3 (EPI-3). The reference period (REF) was selected to be the previous monthly period before the episodes.

The EPI-1 started at 7 a.m. on 25 April, and the $PM_{2.5}$ concentration reached the daily maximum at 2 p.m. The $PM_{2.5}$ concentrations remained elevated until 29 April, and reached a maximum value of 52.9 $\mu g\,m^{-3}$ on 26 April. A short period of lower $PM_{2.5}$ concentrations lasted for a day and a half, and on 1 May concentrations increased again. During the EPI-2, the $PM_{2.5}$ concentrations were

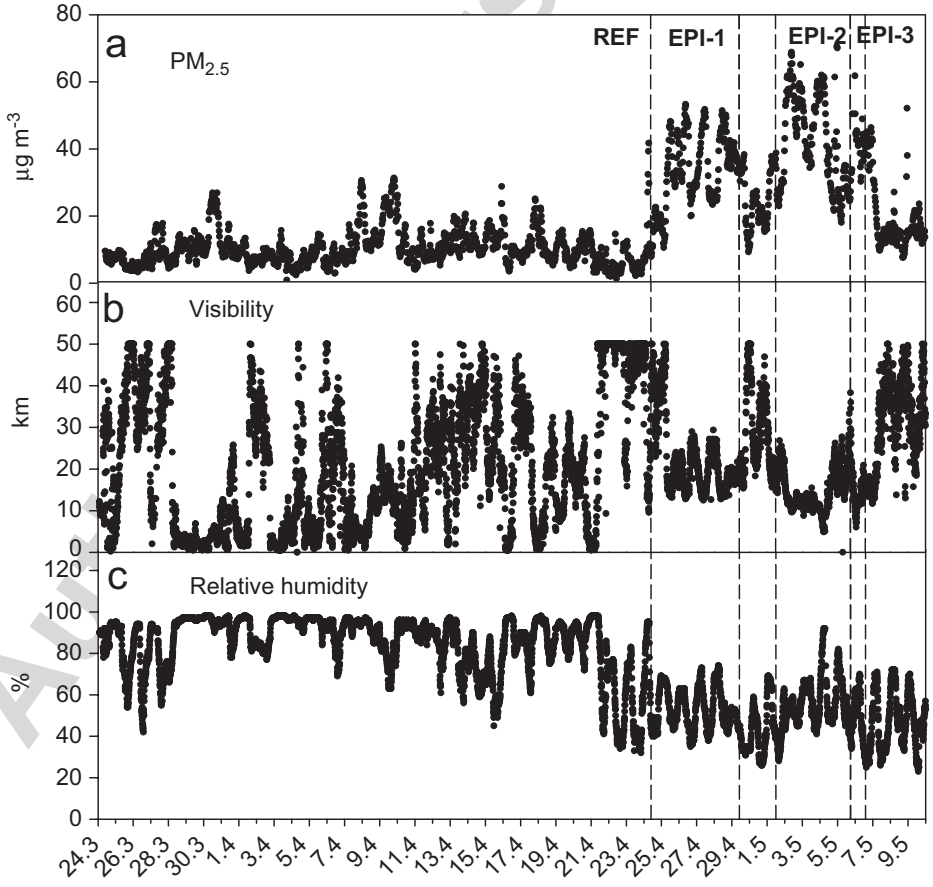


Fig. 1. The concentrations of $PM_{2.5}$ (a), visibility (b) and relative humidity (c) in the reference period (REF) and during three episodes (EPI-1–3). The durations of the episodes were chosen on the basis of $PM_1$ filter samplings.

even higher than during the EPI-1 with the highest concentration of 68.8 $\mu g\,m^{-3}$ on 2 May.

The EPI-3 is difficult to characterize due to the local warehouse fire event. On 5 May around 7:30 p.m., a warehouse fire started in central Helsinki at a distance of 5 km south of the SMEAR III. During the warehouse fire, the wind direction was mostly from the north, but varied substantially. The wind speed was low (0–1.7 $m\,s^{-1}$). Although the warehouse fire was extinguished by the morning of 6 May, the $PM_{2.5}$ concentration remained high until 7 May. This is an indication that the long-range transport episode still probably influenced the $PM_{2.5}$ concentrations on 5–7 May. This paper focuses on the analysis of the long-range transported episodes EPI-1 and EPI-2, as the EPI-3 was caused partly by long-range transported pollution and partly by the local fire emissions.

### 3.1.2. Locally measured meteorological parameters

Fig. 1b and c presents the visibility and relative humidity before and during the course of the episodes. The visibility decreased remarkably both at the beginning of the EPI-1 and the EPI-2 and it remained at a steadily low level for an extensive period. The visibility was also low during the reference period, but those cases were commonly accompanied with high relative humidity, which indicates fog or precipitation situations. On the contrary, during episodes the relative humidity was constantly low even at night.

### 3.1.3. Ions and black carbon

Concurrent with $PM_{2.5}$, the concentrations of biomass burning tracers, potassium and oxalate, increased during the episodes (Fig. 2a and b). In case of black carbon, the concentrations were higher during the episodes than in the REF, however, they were also affected by the diurnal variation of traffic emissions similarly as in non-episodic conditions (Fig. 2c). To minimize the effect of local traffic, the biomass burning contribution to black carbon concentrations have been roughly estimated on the basis of its concentration baseline. The baseline is

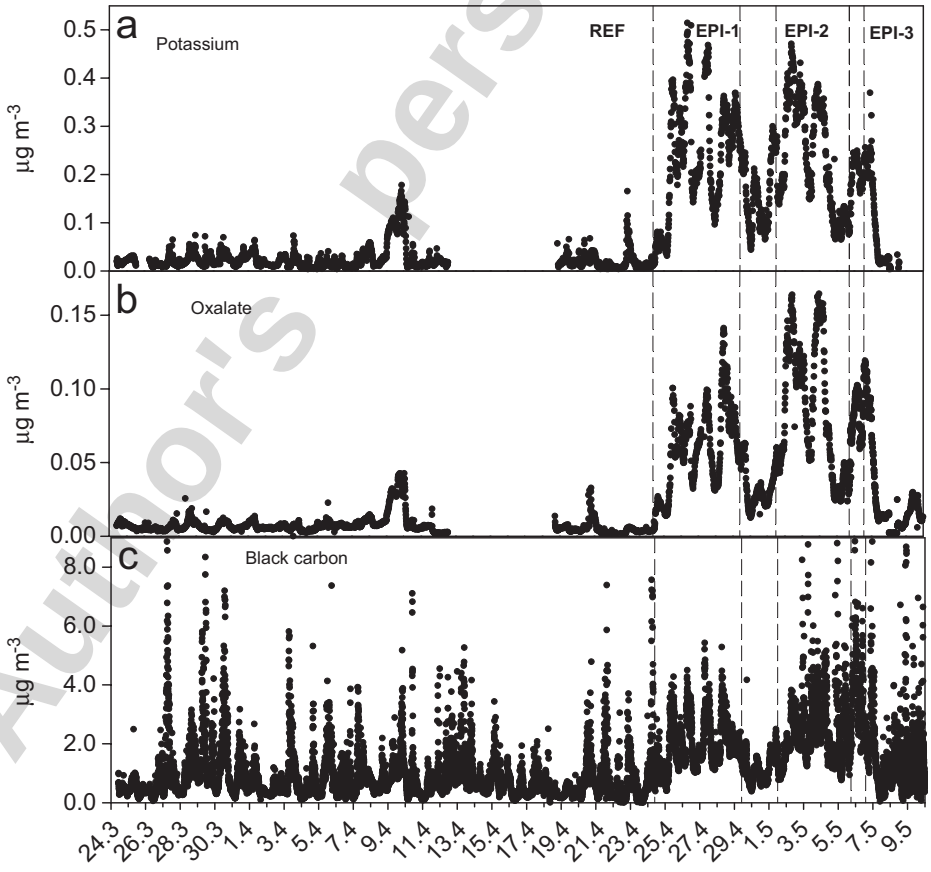


Fig. 2. The concentrations of potassium (a), oxalate (b) and black carbon (c) during the reference period (REF) and three episodes (EPI-1–3). (a) and (b) were measured using the PILS-IC and (c) with the aethalometer. The durations of the episodes were chosen on the basis of $PM_1$ filter samplings.

Table 1
The concentrations (mean ± SD) during the reference period (REF, from 24 March to 24 April) and the episodic periods (EPI-1, 24–29 April and EPI-2, 1–5 May), and their concentration ratios (EPI-to-REF ratio). The values have been presented for fine and coarse particulate matter (TEOM), and for several chemical components analysed from $PM_1$ filters. The number of data points ($n$) for the REF, EPI-1 and EPI-2 periods are 19, 8 and 8, respectively.

| Component | $\mu g\,m^{-3}$ | | | EPI-to-REF concentration ratio | |
|---|---|---|---|---|---|
| | REF | EPI-1 | EPI-2 | EPI-1 | EPI-2 |
| $PM_{2.5}$ | 10.0 ± 3.0 | 36 ± 9.6 | 43 ± 11 | 3.6 | 4.3 |
| $PM_{2.5–10}$ | 8.9 ± 9.1 | 29 ± 9.4 | 38 ± 15 | 3.2 | 4.2 |
| OC | 1.3 ± 0.45 | 11 ± 3.3 | 9.7 ± 4.0 | 8.5 | 7.7 |
| WSOC | 0.72 ± 0.27 | 6.3 ± 2.1 | 6.6 ± 2.7 | 8.7 | 9.1 |
| WISOC | 0.54 ± 0.29 | 4.4 ± 1.4 | 3.2 ± 1.4 | 8.2 | 5.8 |
| EC | 0.59 ± 0.24 | 2.4 ± 0.97 | 2.5 ± 0.94 | 4.1 | 4.2 |
| Levoglucosan | 0.032 ± 0.019 | 0.29 ± 0.12 | 0.22 ± 0.14 | 8.9 | 6.7 |
| Sulphate | 1.8 ± 0.54 | 2.4 ± 0.31 | 4.9 ± 1.4 | 1.3 | 2.7 |
| Potassium | 0.042 ± 0.017 | 0.30 ± 0.11 | 0.29 ± 0.12 | 7.0 | 6.8 |
| Oxalate | 0.050 ± 0.019 | 0.31 ± 0.093 | 0.37 ± 0.13 | 6.2 | 7.4 |

determined as a minimum of the hourly averages of the day. This approach gives a baseline level of $0.28\,\mu g\,m^{-3}$ for the REF, $1.0\,\mu g\,m^{-3}$ for the EPI-1 and $1.3\,\mu g\,m^{-3}$ for the EPI-2. The REF-to-EPI-ratios are in accordance with the corresponding ratio achieved for EC (Table 1). There was a gap in potassium and oxalate data during 12–19 April caused by a pause in the measurements of the PILS-IC system. The absence of potassium data after the episodes resulted from its concentrations being below the detection limit.

### 3.2. Chemical composition of particulate matter

The chemical composition of fine particles before and during the episode was studied in more detail using 12–24 hourly filter samples. The average values of the $PM_{2.5}$ and $PM_{2.5–10}$, and the concentrations of chemical constituents in $PM_1$ before and during the episodes have been presented in Table 1. The third episode (EPI-3) is not considered here, due to the low number of data ($n = 1$) during that period. During the REF, the concentrations of various chemical components were fairly constant even though there were a few short periods of slightly elevated concentrations of $PM_{2.5}$ (see Fig. 1a). The mean (±SD) $PM_{2.5}$ concentration in the REF ($10.0 \pm 3.0\,\mu g\,m^{-3}$, Table 1) is comparable to the annual mean urban background $PM_{2.5}$ concentration ($7.8\,\mu g\,m^{-3}$ in 2001) measured in Helsinki (Sillanpää et al., 2006).

During the EPI-1, the episode-to-reference ratio was highest for levoglucosan, which is a specific tracer for biomass combustion (Simoneit et al., 1999). The corresponding ratio for the other two tracers, potassium and oxalate, was slightly lower compared with that of levoglucosan. The OC and its subfractions WSOC and WISOC were substantially elevated during both episodes, whereas for EC the episode-to-reference ratios were lower than for WSOC and WISOC during both the episodes. Sulphate concentration was substantially increased during the EPI-2, but only slightly increased during the EPI-1. For the other measured ions, chloride, nitrate, sodium, ammonium, magnesium and calcium, the episodes could not be distinguished from the reference period. The $PM_{2.5}$ concentrations were relatively more elevated during the episodes compared with the corresponding ratios for $PM_{2.5–10}$.

### 3.3. Chemical mass closure of fine particles

Chemical mass closure was constructed for the reference period and the episodes by summing up all the inorganic ions, particulate organic matter and EC analysed from the $PM_1$ samples. Corresponding particle mass was obtained from the TEOM. A non-volatile mass, which constitutes on average 86 ± 5.8% of total mass of the TEOM, was used for the mass closure calculations since the semi-volatile fraction was assumed to be lost prior to the chemical analyses in $PM_1$ samples. The chemical composition and chemical mass closure of fine particles is presented in Fig. 3a. The mass closure of carbonaceous particulate matter is shown separately in Fig. 3b.

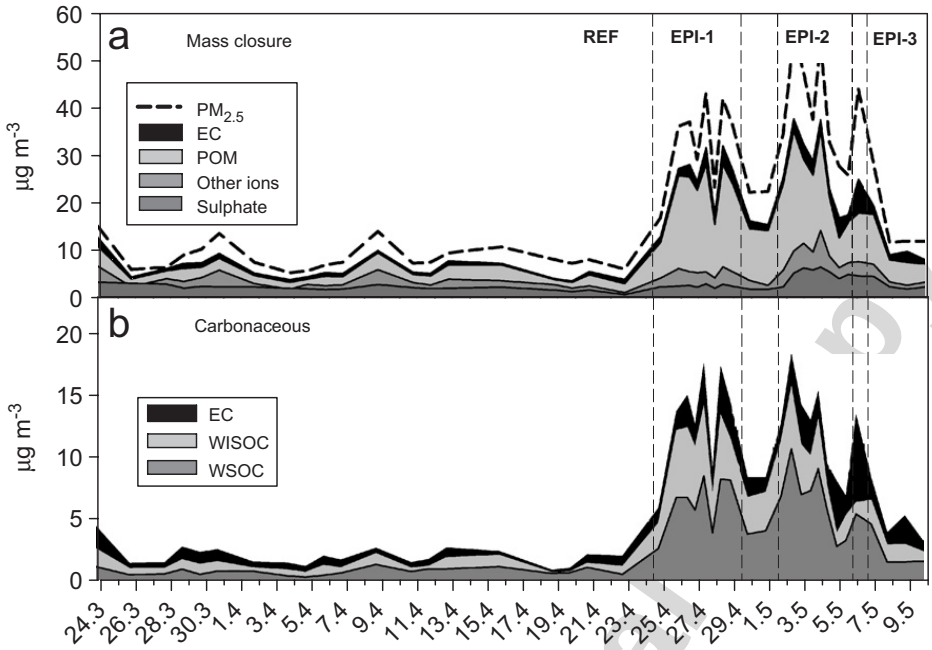


Fig. 3. Mass closure for fine particles (a) and the composition of its carbonaceous fraction (b) prior and during the episodes in Helsinki. $PM_{2.5}$ was measured with the TEOM whereas all the chemical components were analysed from the $PM_1$ filters. REF and EPI-1–3 stand for the reference period and the episodes 1–3.

The sum of chemical components in $PM_1$ accounted on average ($\pm$SD) for $71\pm11\%$ in the REF, $76\pm3.3\%$ in the EPI-1 and $69\pm4.7\%$ in the EPI-2 of the total $PM_{2.5}$ mass. The contribution of POM to $PM_{2.5}$ increased during both the episodes, whereas that of measured inorganic ions decreased. These changes have been presented in more detail in Fig. 4a. On average, POM accounted for $25\pm5.4\%$ of $PM_{2.5}$ during the REF, while during the EPI-1 and EPI-2, the contribution of POM was $52\pm4.5\%$ and $39\pm9.0\%$, respectively. On the contrary, the mean contribution ($\pm$SD) of inorganic ions to $PM_{2.5}$ was $30\pm6.7\%$ during the REF, but during the EPI-1 and EPI-2, it decreased to $15\pm3.0\%$ and $21\pm3.6\%$, respectively.

WSOC accounted for $40\pm14\%$, $48\pm4.2\%$ and $52\pm8.6\%$ of carbonaceous mass (OC + EC) during the REF, EPI-1 and EPI-2, respectively, whereas WISOC accounted for $28\pm10\%$, $34\pm5.7\%$ and $25\pm6.5\%$ of that mass during the same periods. Although the mean proportion of WSOC to total carbon was higher during the episodes, the difference is within the standard deviation of the WSOC-to-OC ratio in the REF. The WSOC-to-OC ratio is represented in more detail in Fig. 4b. The rest of the carbon was composed of EC with slightly higher proportion during the REF than the EPI-1 and EPI-2. However, during the local warehouse fire (EPI-3), half of the carbon was composed of EC.

### 3.4. Predicted concentrations and their comparison to measured values

The spatial distribution of the modelled mean emission flux of $PM_{2.5}$ from fires is presented in Fig. 5, as an average over the 25-day period from 20 April to 15 May 2006 (EPI-1–3). The fires cover an extensive area in the western parts of Russia, in the immediate vicinity of the Baltic countries, Belarus and Ukraine. An example of the predicted results, using the HIRLAM meteorological data, is shown in Fig. 5. In Fig. 5, the spatial hourly $PM_{2.5}$ concentration distribution originating from the fires is presented for one selected hour (27 April 2006 at 12:00 UTC). The plume is located over an extensive geographical area from the Black Sea to Spitsbergen in the north (the latter not shown in the figure).

A comparison of the modelled $PM_{2.5}$ concentrations from the fires with the measured $PM_{2.5}$ concentrations is presented in Fig. 6. Qualitatively, the model has succeeded well in predicting the EPI-1 and EPI-3, but it has mostly missed the EPI-2. To investigate the reason and delineate the source areas responsible for this episode, adjoint simulations using the SILAM model for the EPI-2 have been

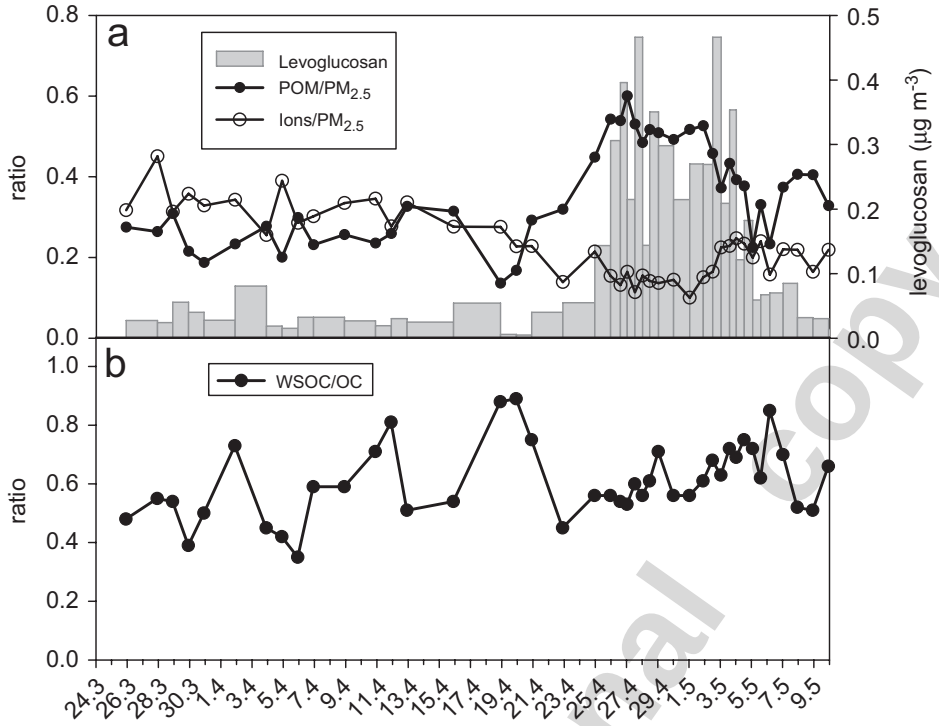




Fig. 4. POM-to-$PM_{2.5}$ and inorganic ions-to-$PM_{2.5}$ ratios (lines) and the concentration of levoglucosan (bars) (a), and the WSOC-to-OC ratio (b). $PM_{2.5}$ was measured with the TEOM whereas all the chemical components were analysed from the $PM_1$ filters.

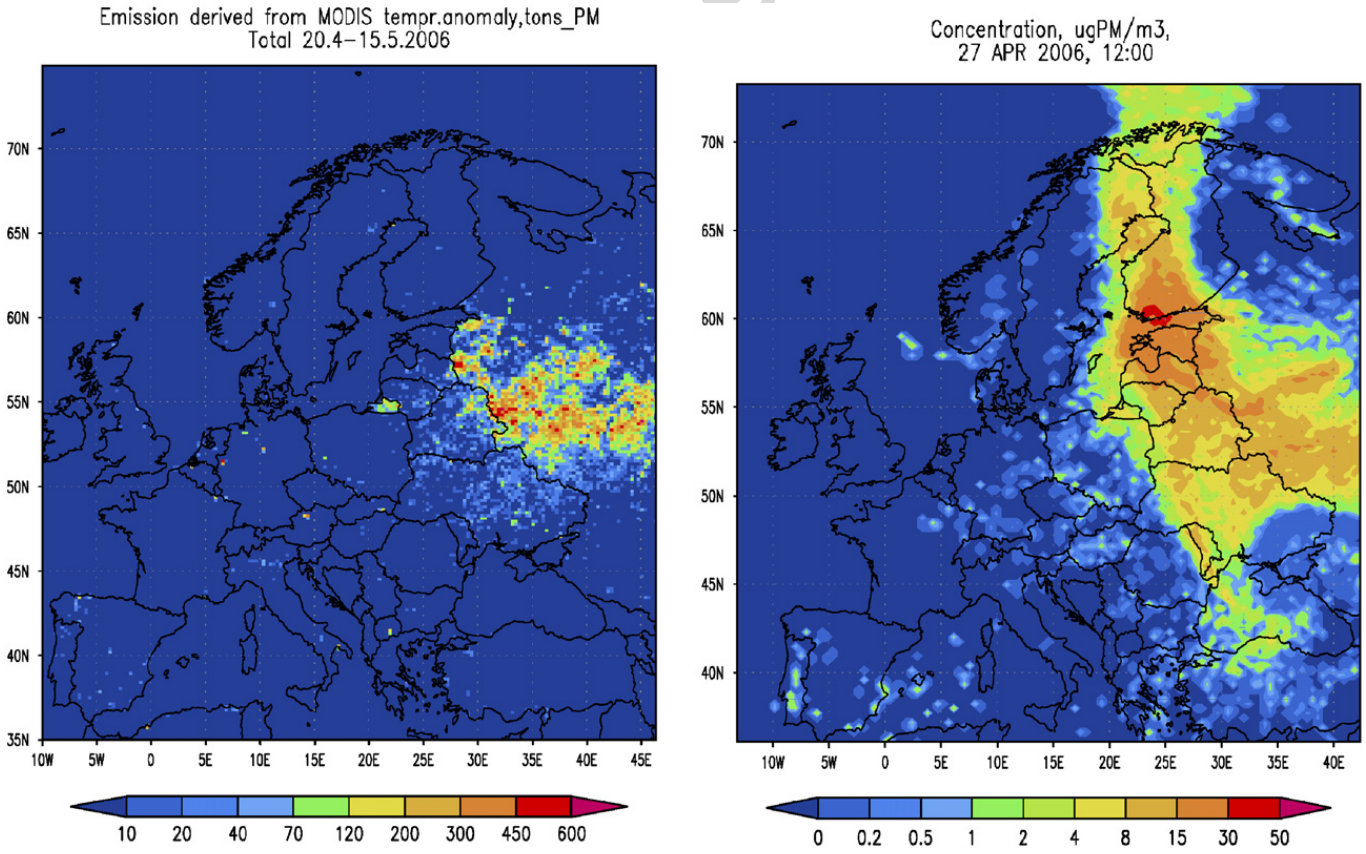


Fig. 5. The mean predicted $PM_{2.5}$ emission flux originated from fires during 20 April–15 May 2006, computed based on the measured MODIS temperature anomalies (left-hand panel, unit: tonnes PM), and $PM_{2.5}$ concentrations over Europe at 12:00 (UTC), 27 April 2006 (right-hand panel, unit: $\mu g\,m^{-3}$).

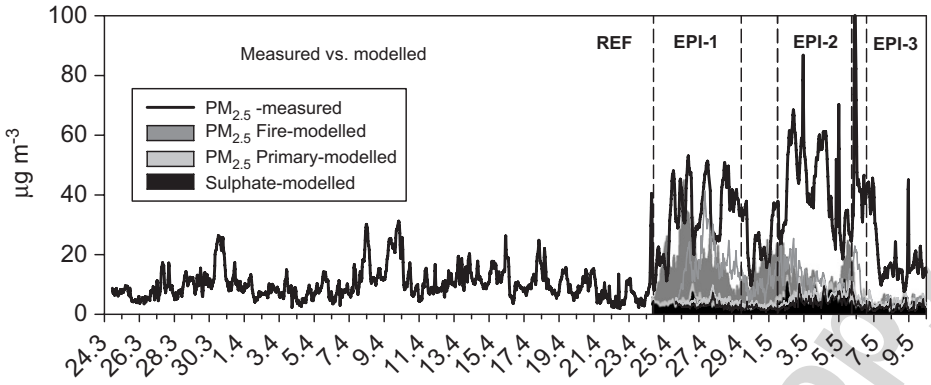


Fig. 6. The comparison between measured $PM_{2.5}$ and modelled $PM_{2.5}$. $PM_{2.5}$-measured was determined with the TEOM and Fire-modelled refers to $PM_{2.5}$ originated from fires, Primary-modelled to anthropogenic $PM_{2.5}$ from primary sources other than fires and Sulphate-modelled to sulphate concentrations.

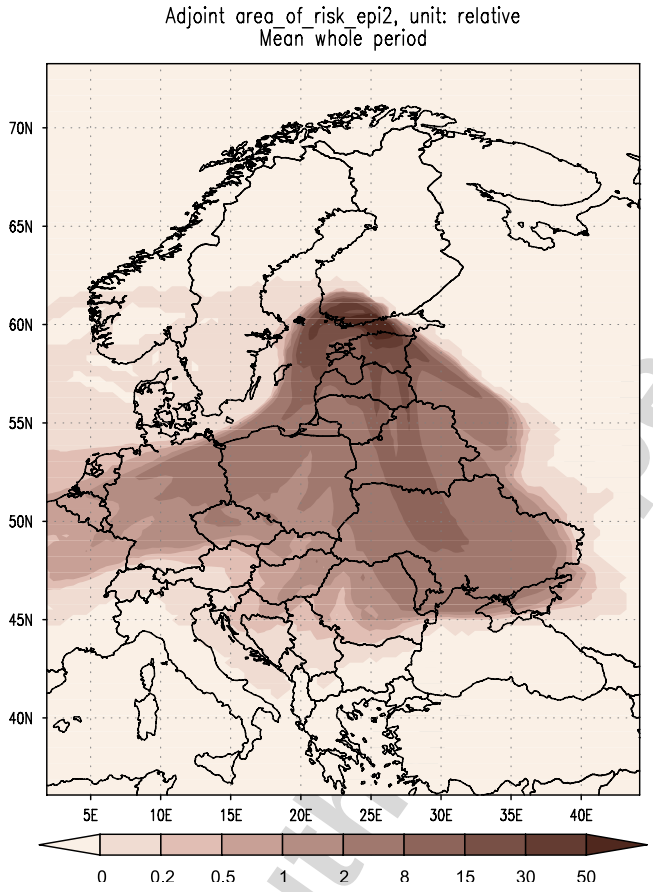


Fig. 7. A source-apportioning spatial probability distribution computed by SILAM for the EPI-2 observed in Helsinki (1–5 May 2006). Relative units.

performed. The model was provided with observational data as emission input (monitoring station represented as a point source) and then used to solve the adjoint dispersion equation backward in time. The resulting "footprint" (Fig. 7) can be considered as a probability distribution for the sources that caused the observed concentrations. Sources outside the footprint area had not affected the Helsinki site during EPI-2. The most probable source areas for this event are located to the west, and also partially to the north of the main observed burning region (Fig. 7). However, contribution of the main area was also non-negligible.

## 4. Discussion

The episode of elevated $PM_{2.5}$ concentration started on 24 April and lasted for almost 2 weeks. Modelling of the $PM_{2.5}$ concentrations showed that most of the particles were long-range transported from the western parts of Russia where widespread fires were observed. The real-time measurements of biomass burning tracers, i.e., potassium and oxalate, showed that these compounds had a similar temporal evolution to the concentration of $PM_{2.5}$ confirming a biomass burning origin of the episodes. The concentration of the third tracer compound considered, levoglucosan, was also found to increase remarkably during the episodes.

The duration of these episodes was exceptionally long compared with the episodes of long-range transport detected earlier in southern Finland. In 2002, the $PM_{2.5}$ concentrations increased over a 5-day-long period in March and the series of 2–4-day-long episodes occurred in August and September (Niemi et al., 2004, 2005). In this study, the tracers for biomass burning, potassium and oxalate, were measured continuously with a high temporal resolution; therefore, the data are better suited for studying the biomass burning episodes than previously (Sillanpää et al., 2005).

According to MODIS data, there are wild land fires in Russia, Belarus and Ukraine happening every year. These commonly start in March, and the number of fires is largest in April. The intensity of these fires varies from year to year, which is caused largely by meteorological conditions in spring, such as the occurrence of precipitation, the temperature, etc. Wild land fires occur also in summer and in autumn, but typically these are less widespread. For the episode detected in Finland in March 2002, a burn of agricultural land was proposed for the origin of fires (Niemi et al., 2004). Agricultural biomass combustion extends easily to wild lands fires, both of which were probably the sources of the episodes detected in Finland in 2006. In this study, the type of the fire could not be specified. Different types of man-made fires or wildfires (e.g., forest fires, agricultural waste combustion, flaming and smoldering) have different emission profiles (Conny and Slater, 2002; Hays et al., 2005), but due to the long transportation time, the chemical composition of emitted particles may change.

The dispersion of fire plumes and resulting episodes, their severity, duration and affected areas depend on meteorological conditions. For the current episode, the dispersion simulations showed that its exceptionally long duration was caused by a long-lasting anti-cyclonic system over western Russia, which caused the fire fumes to be transported northwards of the burning region for almost a week. The fires themselves started considerably earlier, but were extinguished at the end of the episode by the atmospheric front, which both altered dispersion conditions (in particular, transport direction) and sharply reduced the source areas.

### 4.1. Chemical composition

Excluding sulphate, the average chemical composition of the particles during the long-range transport episodes (EPI-1 and EPI-2) was very similar. This suggests that the source category for the EPI-1 and EPI-2 was the same (biomass combustion). The high sulphate concentration during the EPI-2 compared with that in the EPI-1 may be due to the mixing of fire emissions with other anthropogenic pollutants. This was also suggested by the modelled source areas for the EPI-1 and EPI-2 (Fig. 5 and 7), as the source area sector was narrow for the EPI-1, whereas for the EPI-2, it was wider and also contained some parts of the Central Europe.

The chemical mass closure revealed that the contribution of organic components to $PM_{2.5}$ was remarkably higher during the episodes than during the reference period. Quite surprisingly, the contribution of WSOC and biomass burning tracers to OC did not change significantly from the reference period to the episodes. This could imply that during the REF, the major emission source for OC was quite similar to that of the episode. In Finland and northern Europe, this is most likely related to local and regional wood combustion or, alternatively, a continuous contribution of long-range transported biomass burning emissions to the OC concentrations also in the reference period.

In this study, the chemical mass closure was constructed with the continuous $PM_{2.5}$ mass measurements (TEOM) and the chemical composition from the $PM_1$ filter samples. This procedure was chosen because quartz fibre filters, used for the $PM_1$ sampling, are difficult to weigh accurately. Also the contamination risk before the chemical analysis was minimized. Around 70% of the particle mass was determined by the chemical analyses. The large part of the unidentified fraction was due to the mass between $PM_1$ and $PM_{2.5}$ that was not collected on the $PM_1$ filters and therefore it was not analysed chemically.

The mass closure requires the conversion of the mass of OC to that of organic matter. Since there was no instrument to measure this value directly, a general multiplication factor of 1.6 was used as suggested by Turpin and Lim (2001). They recommended a higher factor (2.2–2.6) for aerosol heavily impacted by wood smoke, which may result in an underestimated value for the POM in this work. Also, the measured concentrations of OC and WSOC can be considered as the minimums, since the measurement system takes into account the positive artefact (adsorption of gas-phase organic compounds on quartz filter), but excludes the negative artefact (evaporation of semi-volatile compounds from the front filter).

### 4.2. Modelling

The modelling succeeded best in predicting the episodes EPI-1 and EPI-3. For the EPI-1, the modelled values even reached a quantitatively good agreement with the observed peak concentrations. Concentrations during the EPI-3 were underpredicted, which is to be expected, as the major source of this episode was the local warehouse fire.

The plume from this fire was narrow when it reached the measurement site (about 5 km straight downwind, which roughly corresponds to less than 1 km of width of the plume). The model grid cell is $20 \times 20\,km^2$, which implies much larger dilution and, consequently, underestimation of the concentrations.

The predictions missed EPI-2 almost completely. The most probable reason was that the burning region was covered by the dense frontal clouds since the beginning of May and the fire was not detected by MODIS. In this study, we did not introduce any correction to this failure to detect the fire. When the front passed the suspected burning area, MODIS did not report the fires any more probably because they were extinguished by the frontal rains.

Measured particles during the EPI-2 may originate from some other burning region, which was located closer to Helsinki but missed by MODIS, possibly due to clouds. This possibility was investigated by performing adjoint SILAM model computations, the results of which are presented in Fig. 7. The most probable source areas for the EPI-2 peak are to the west and north of the main burning region. However, the main region has non-negligible contribution as well. Resolving this issue conclusively would require more satellite- or ground-based forest fire data from Eastern Europe and Baltic countries.

## 5. Conclusions

The near-real-time instruments used in this study revealed the episodes in detail, which provided a valuable tool for the comparisons with the $PM_{2.5}$ models. According to the model simulations, MODIS successfully detected the fires that caused the first set of concentration peaks (EPI-1) and the local warehouse fire (EPI-3), but missed the second pollution episode (EPI-2), probably due to dense frontal clouds. However, the results from chemical analyses suggested that the source of the EPI-1 and EPI-2 was similar, even though the model computations show that the most probable source sector was wider for the EPI-2. This could explain the increased sulphate concentration during the EPI-2, compared with that during EPI-1, since the source area for the EPI-2 included also areas from Central Europe. Based on the MODIS data, most of the fires that caused the episodes EPI-1 and EPI-2 were situated in western Russia.

The MODIS monthly fire maps, available since 2001, showed that these episodes of biomass combustion in March–April occur annually. However, the duration, geographical extent and concentrations of the particulate matter pollution from these fires were exceptional in spring 2006. This was caused by specific meteorological conditions that resulted in the transport of the fire plumes well beyond the northern continental Europe up to high Arctic latitudes. The analysis of the fire plumes performed in this study, especially regarding the chemical composition of aerosols, can therefore be utilized in other studies that investigate the health effects or climatic influence of biomass burning.

## Acknowledgements

Financial support from the Finnish Funding Agency for Technology and Innovation (Grant no. 40531/04, and the KOPRA project), the Academy of Finland (Contract no. 201131) and the Maj and Tor Nessling Foundation is gratefully acknowledged. Authors also thank Prof. David Schultz for his comments and for the revision of the English language.

## References

Allen, G., Sioutas, C., Koutrakis, P., Reiss, R., Lurmann, F.W., Roberts, P.T., 1997. Evaluation of the TEOM® method for measurement of ambient particulate mass in urban areas. Journal of the Air and Waste Management Association 14, 682–689.

Andreae, M.O., Merlet, P., 2001. Emission of trace gases and aerosols from biomass burning. Global Biogeochemical Cycles 15, 955–966.

Berner, A., Lürzer, C., 1980. Mass size distributions of traffic aerosols at Vienna. Journal of Physical Chemistry 84, 2079–2083.

Birch, M.E., Cary, R.A., 1996. Elemental carbon-based method for monitoring occupational exposures to particulate diesel exhaust. Aerosol Science and Technology 25, 221–241.

Conny, J.M., Slater, J.F., 2002. Black carbon and organic carbon in aerosol particles from crown fires in the Canadian boreal forest. Journal of Geophysical Research 107, D11.

Debell, L.J., Talbot, R.W., Dibb, J.E., Munger, J.W., Fischer, E.V., Frolking, S.E., 2004. A major regional air pollution event in the northeastern United States caused by extensive forest fires in Quebec, Canada. Journal of Geophysical Research 109, D19305.

Duclos, P., Sanderson, L.M., Lipsett, M., 1990. The 1987 forest fire disaster in California: assessment of emergency room visits. Archives of Environmental Health 45, 53–58.

Dye, C., Yttri, K.E., 2005. Determination of monosaccharide anhydrides in atmospheric aerosols by use of high-performance

liquid chromatography combined with high-resolution mass spectrometry. Analytical Chemistry 77, 1853–1858.

Fine, P.M., Cass, G.R., Simoneit, B.R.T., 2001. Chemical characterization of fine particle emissions from fireplace combustion of woods grown in the Northeastern United States. Environmental Science and Technology 35, 2665–2675.

Fraser, M.P., Lakshmanan, K., 2000. Using levoglucosan as a molecular marker for the long-range transport of biomass combustion aerosols. Environmental Science and Technology 34, 4560–4564.

Giglio, L., van der Werf, G.R., Randerson, J.T., Collatz, G.J., Kasibhatla, P.S., 2006. Global estimation of burned area using MODIS active fire observations. Atmospheric Chemistry and Physics 6, 957–974 SRef-ID: 1680-7324/acp/2006-6-957.

Hansen, A.D.A., Rosen, H., Novakov, T., 1984. The aethalometer: an instrument for the real-time measurement of optical absorption by aerosol particles. Science of the Total Environment 36, 191–196.

Hays, M.D., Fine, P.M., Geron, C.D., Kleeman, M.J., Gullett, B.K., 2005. Open burning of agricultural biomass: Physical and chemical properties of particle-phase emissions. Atmospheric Environment 39, 6747–6764.

Heil, A., Goldammer, J.G., 2001. Smoke-haze pollution: a review of the 1997 episode in Southeast Asia. Regional Environmental Change 2, 24–37.

Jaffrezo, J.-L., Davidson, C.I., Kuhns, H.D., Bergin, M.H., Hillamo, R., Maenhaut, W., Kahl, J.W., Harris, J.M., 1998. Biomass burning signatures in the atmosphere of central Greenland. Journal of Geophysical Research D 23, 31,067–31,078.

Karppinen, A., Härkönen, J., Kukkonen, J., Aarnio, P., Koskentalo, T., 2004. Statistical model for assessing the portion of fine particulate matter transported regionally and long range to urban air. Scandinavian Journal of Work, Environment and Health 30 (Suppl. 2), 47–53.

Loo, B.W., Cork, C.P., 1988. Development of high efficiency virtual impactor. Aerosol Science and Technology 9, 167–170.

Metzger, K.B., Tolbert, P.E., Klein, M., Peel, J.L., Flanders, W.D., Todd, K., Mulholland, J.A., Ryan, P.B., Frumkin, H., 2004. Ambient air pollution and cardiovascular emergency department visits. Epidemiology 15, 46–56.

Niemi, J.V., Tervahattu, H., Vehkamäki, H., Kulmala, M., Koskentalo, T., Sillanpää, M., Rantamäki, M., 2004. Characterization and source identification of a fine particle episode in Finland. Atmospheric Environment 38, 5003–5012.

Niemi, J.V., Tervahattu, H., Vehkamäki, H., Martikainen, J., Laakso, L., Kulmala, M., Aarnio, P., Koskentalo, T., Sillanpää, M., Makkonen, U., 2005. Characterization of aerosol particle episodes in Finland caused by wildfires in Eastern Europe. Atmospheric Chemistry and Physics 5, 2299–2310.

Orsini, D.A., Ma, Y., Sullivan, A., Sierau, B., Baumann, K., Weber, R.J., 2003. Refinements to the particle-into-liquid sampler (PILS) for ground and airborne measurements of water soluble aerosol composition. Atmospheric Environment 37, 1243–1259.

Pakkanen, T.A., Kerminen, V.-M., Korhonen, C.H., Hillamo, R.E., Aarnio, P., Koskentalo, T., Maenhaut, W., 2001. Use of atmospheric elemental size distributions in estimating aerosol sources in the Helsinki area. Atmospheric Environment 35, 5537–5551.

Patashnick, H., Rupprecht, E.G., 1991. Continuos PM-10 measurements using the Tapered Element Oscillating Micro-Balance. Journal of the Air and Waste Management Association 41, 1079–1083.

Seinfeld, J.H., Pandis, S.N., 1998. Atmospheric Chemistry and Physics: From Air Pollution to Climate Change. Wiley, New York.

Sillanpää, M., Saarikoski, S., Hillamo, R., Pennanen, A., Makkonen, U., Spolnik, U., Van Grieken, R., Koskentalo, T., Salonen, R.O., 2005. Chemical composition, mass size distribution and source analysis of long-range transported wildfire smokes in Helsinki. Science of the Total Environment 350, 119–135.

Sillanpää, M., Hillamo, R., Saarikoski, S., Frey, A., Pennanen, A., Makkonen, U., Spolnik, Z., Van Grieken, R., Braniš, M., Brunekreef, B., Chalbot, M.-C., Kuhlbusch, T., Sunyer, J., Kerminen, V.-M., Kulmala, M., Salonen, R.O., 2006. Chemical composition and mass closure of particulate matter at six urban sites in Europe. Atmospheric Environment 40S2, 212–223.

Simoneit, B.R.T., Schauer, J.J., Nolte, C.G., Oros, D.R., Elias, V.O., Fraser, M.P., Rogge, W.F., Cass, G.R., 1999. Levoglucosan, a tracer for cellulose in biomass burning and atmospheric particles. Atmospheric Environment 33, 173–182.

Sofiev, M., Siljamo, P., Valkama, I., Ilvonen, M., Kukkonen, J., 2006. A dispersion modelling system SILAM and its evaluation against ETEX data. Atmospheric Environment 40, 674–685.

Turpin, B.J., Lim, H.-J., 2001. Species contributions to $PM_{2.5}$ mass concentrations: revisiting common assumptions for estimating organic mass. Aerosol Science and Technology 35, 602–610.

Watson, J.G., Chow, J.C., Lu, Z., Fujita, E.M., Lowenthal, D.H., Lawson, D.R., 1994. Chemical mass balance source apportionment of $PM_{10}$ during the Southern California air quality study. Aerosol Science and Technology 21, 1–36.